ISSN: 2476-6909; Modares. Mech. Eng. *2026;26(09):743-755.*

Modares Mechanical Engineering

DOI: 10.48311/mme.2026.119007.82968
journal homepage: mme.modares.ac.ir

Experimental Investigation of Pilot Whole-Body Vibrations in Helicopters Using Nonlinear Dynamic Modeling of Polyurethane Seat Cushion

Seyed Mohammad Kamali[1], Ali Nouri[1*], Heshmat Allah Mohammad Khanlo[1], Hadi sabouri[2]

[1] Department of Aerospace Engineering, Shahid Sattari Aeronautical University of Science and Technology, Tehran, Iran
[2] Faculty of Engineering, Department of Mechanical Engineering, Kharazmi University, Tehran, Iran

ARTICLE INFO

Article Type
Original Research

Article History
Received: January 31, 2026
Revised: February 19, 2026
Accepted: March 15, 2026
ePublished: June 27, 2026

ABSTRACT

Exposure to helicopter vibrations during flight and maneuvers can lead to long-term physical strain on pilots, particularly in the low-frequency range (0–20 Hz). While seat suspensions provide some vibration isolation, the seat cushion plays a critical role in overall ride comfort. This study presents an integrated computational and experimental investigation of nonlinear polyether polyurethane seat cushions and their effect on helicopter pilot comfort. Ride comfort is initially analyzed using a 4-DOF biodynamic model and subsequently extended to a 5-DOF model to explicitly include seat cushion dynamics. Experimental measurements of both linear and nonlinear stiffness and damping properties are conducted through modal analysis tests, providing data for model validation. Results demonstrate that considering nonlinear cushion behavior significantly improves predictions of transmissibility, mechanical impedance, and apparent mass, showing strong agreement with experimental observations. The findings highlight the importance of accurate nonlinear modeling for the design of seat cushions that enhance vibration isolation and improve overall pilot ride comfort.

Keywords: Cushion, ride comfort, Whole body vibration, Transmissibility, Nonlinear Damping and Stiffness

How to cite this article
Kamali S. M., Nouri A., Mohammad Khanlo H.A, Sabouri H., Experimental Investigation of Pilot Whole-Body Vibrations in Helicopters Using Nonlinear Dynamic Modeling of Polyurethane Seat Cushion. Modares Mechanical Engineering; Eng. *2026;26(09):743-755.*

*Corresponding author's email: nouri@ssau.ac.ir
*Corresponding ORCID ID: 0000-0002-2080-6306

شاپا: ۶۹۰۹-۲۴۷۶؛ مهندسی مکانیک مدرس. ۷۵۵-۷۴۳:(۰۹)۱۴۰۵;۲۶

مهندسی مکانیک مدرس

DOI: 10.48311/mme.2026.119007.82968

صفحه اصلی مجله: mme.modares.ac.ir

بررسی تجربی ارتعاشات وارد بر بدن خلبانان بالگرد با مدلسازی رفتار دینامیکی غیرخطی بالشتک صندلی پلی‌یورتان

سید محمد کمالی[۱]، علی نوری[۱*]، حشمت الله محمد خانلو[۱]، هادی صبوری[۲]

[۱]دانشکده مهندسی هوافضا، دانشگاه علوم و فنون هوایی شهید ستاری، تهران، ایران

[۲] گروه مهندسی مکانیک، دانشکده مهندسی، دانشگاه خوارزمی، تهران، ایران

اطلاعات مقاله

نوع مقاله

مقاله پژوهشی

تاریخچه مقاله

دریافت: ۱۴۰۴/۱۱/۱۱

بازنگری: ۱۴۰۴/۱۱/۳۰

پذیرش: ۱۴۰۴/۱۲/۲۴

ارائه آنلاین: ۱۴۰۵/۰۴/۰۶

چکیده

ارتعاشات ناشی از پرواز و مانورهای بالگرد، به‌ویژه در محدوده فرکانسی پایین (۰ تا ۲۰ هرتز)، می‌توانند موجب بروز تنش‌های فیزیکی بلندمدت و کاهش راحتی خلبان شوند. اگرچه سامانه‌های تعلیق صندلی نقش مؤثری در کاهش انتقال ارتعاشات ایفا می‌کنند، عملکرد بالشتک صندلی به‌عنوان یکی از عوامل کلیدی در بهبود راحتی پرواز شناخته می‌شود. در این پژوهش، یک رویکرد یکپارچه محاسباتی–تجربی برای بررسی تأثیر بالشتک‌های غیرخطی پلی‌اورتان پلی‌اتر بر راحتی خلبان بالگرد ارائه شده است. به‌منظور ارزیابی پاسخ بیودینامیکی، ابتدا یک مدل چهار درجه آزادی توسعه یافت و سپس با افزودن دینامیک بالشتک صندلی، مدل به یک سامانه پنج درجه آزادی گسترش داده شد. پارامترهای سختی و میرایی خطی و غیرخطی بالشتک‌ها از طریق آزمون‌های تجربی تحلیل مودال تعیین و برای اعتبارسنجی مدل‌ها به‌کار گرفته شدند. نتایج نشان داد که در نظر گرفتن رفتار غیرخطی بالشتک صندلی، دقت پیش‌بینی شاخص‌های انتقال‌پذیری، امپدانس مکانیکی و جرم ظاهری را به‌طور قابل‌توجهی بهبود می‌بخشد و انطباق مناسبی با داده‌های تجربی دارد. یافته‌های این مطالعه بر اهمیت مدل‌سازی دقیق رفتار غیرخطی بالشتک‌های صندلی در طراحی سامانه‌های مؤثر ایزولاسیون ارتعاش و ارتقای راحتی خلبانان بالگرد تأکید می‌کند.

کلیدواژه‌ها: بالشتک صندلی بالگرد ، راحتی سرنشین، ارتعاشات کل‌بدنی، انتقال‌پذیری، میرایی و سختی غیرخطی

نحوه ارجاع به این مقاله

کمالی سید محمد، نوری علی، محمد خانلو حشمت الله، صبوری هادی، بررسی تجربی ارتعاشات وارد بر بدن خلبانان بالگرد با مدلسازی رفتار دینامیکی غیرخطی بالشتک صندلی پلی‌یورتان، مهندسی مکانیک مدرس. ۷۵۵-۷۴۳:(۰۹)۱۴۰۵;۲۶

*پست الکترونیکی نویسنده عهده‌دار مکاتبات: nouri@ssau.ac.ir

*شناسه ارکید نویسنده عهده‌دار مکاتبات: ۰۰۰۰-۰۰۰۲-۲۰۸۰-۶۳۰۶

1- Introduction

Helicopters exhibit unique vibration characteristics compared to ground vehicles, primarily due to rotor dynamics and aerodynamic interactions. The main excitation frequencies in helicopters are usually integer multiples of the rotor speed, expressed as N/rev, where N is the number of main rotor blades. In the case of the Bell 214 helicopter, significant excitation frequencies occur at 1, 2 and 4/rev, which are associated with structural vibrations transmitted from the airframe to the pilot's seat. The vibrations of the 214 helicopters are primarily in the 0–20 Hz frequency range, which can have a significant impact on ride comfort and pilot fatigue, and are the source of many health problems such as fatigue and physical injuries to crew and pilot in the long term [1-5].

In studying the effects of vibrations on the human body, researchers have investigated multi-degree-of-freedom models of the seated human body [6]. These models range from a single-degree-of-freedom model to an 11-degree-of-freedom model observed in previous research [7-18]. One of the most important studies was conducted by Griffin and Lewis in 2001, where they replaced parts of the passenger's body with solid masses and investigated 2 and 3 DOF models [10]. Suleiman et al. also used a method to reduce the vehicle suspension system and modeled the vehicle with 7 degrees of freedom (DOF). In addition, this study discusses the comparison between control strategies [17]. Among the multi-degree-of-freedom models, the von Schimmels model is considered one of the best models due to its good agreement with experimental tests [19]. Marzban-Rad et al. studied a biomechanical model of the seated human body to calculate the vertical vibration transmission capability using a genetic algorithm. They introduced two new models, one with and one without support at a certain frequency, to reduce the vibration of the occupant's body [20].

Some studies have specifically focused on the seat suspension system and its effects on reducing vibrations on the human body [21-24]. Furthermore, nonlinear characteristics and constraints of the seat and cushion, similar to saturation effects in dynamic systems, can significantly influence vibration transmission and passenger comfort [25-26]. Heydarian studied the technology and development of the seat suspension system. He concluded that an active suspension system has a greater effect in reducing vibrations to the passenger at low frequencies compared to a semi-active system [27]. Rakhja et al. conducted a review study on the relationship between body vibrations and apparent mass from 1962 to 2008, comparing it with the ISO 5982 standard. Rakheja also demonstrated that approximately 73% of the mass of the human body in a sitting position, with feet on the ground, is supported by the seat, while the remaining weight is borne by the feet [32].

Early investigations on seat cushions and vibration transmission began with Corbridge and Griffin in 1989, who analyzed the effects of vibration intensity, seat type, and position, concluding that passive cushion characteristics predominantly govern body vibration mitigation [33]. Gove and Smith further quantified the influence of cushion material, thickness, and stiffness on vibration attenuation [34,35]. Nonlinear seat cushion dynamics, particularly hysteresis-based stiffness and damping, have been shown to enhance vibration transmissibility predictions, Yin et al. developed a lumped-parameter nonlinear suspension seat model using polynomial approximations from experimental hysteresis data, yielding better agreement with measurements than linear models mirroring the polynomial fitting (Eqs. 9–12) and 5-DOF integration applied here for polyurethane cushions in helicopter pilot applications [36]. Considering that the natural frequency of the upper body and spine lies between 4.8 and 8 Hz [37-39], seat and cushion design strategies focus on minimizing resonance effects within this critical range to enhance pilot comfort.

The superior agreement between experimental data and the nonlinear model predictions (Figs. 20-22) underscores the importance of incorporating hysteresis-derived nonlinearities in cushion modeling. This finding is supported by prior studies on viscoelastic polyurethane foams, where hysteresis fitting and Prony series-based identification significantly improved dynamic response predictions compared to linear assumptions. For example, the relaxation behavior captured in our polynomial fittings aligns with the exponential kernel decompositions used in uniaxial compression tests of flexible foams, while the rate-dependent effects observed in dynamic impedance and apparent mass are consistent with characterizations under transient loading. These enhancements (6.4% in transmissibility, 6.1% in mechanical impedance, and 4.2% in apparent mass) highlight the practical value of nonlinear modeling for optimizing polyurethane seat cushions in high-vibration environments like helicopter cockpits [40-45].

As mentioned in previous sections, studies have shown that a significant amount of research has been conducted on whole body vibration (WBV). However, there has been limited experimental work done to explore ride comfort and the impact of nonlinear damping and stiffness in helicopters with polyurethane seat cushions Previous work by the authors investigated seat suspension and cushion effects on Bell 214 pilot biodynamics using a 4-DOF model. The present study isolates the nonlinear polyurethane cushion (without suspension), providing detailed hysteresis characterization, a 5-DOF model with integrated nonlinear properties, and direct experimental validation on a real pilot [46,47].

In this study, the helicopter ride comfort is first calculated analytically using a 4-degree-of-freedom (4DOF) model, which is then compared and validated against previous experimental models. The linear and nonlinear damping and stiffness of the polyurethane cushion are then determined experimentally .

Furthermore, the ride comfort parameters of the pilot are calculated analytically and experimentally using modal analysis. The results from both the analytical and experimental approaches for helicopter pilot ride comfort are compared. It is important to note that this study focuses on the pilot's seat without a suspension system, and solely investigates the dynamic effects of the cushion on the pilot's comfort.

2- Biodynamic mathematical modeling and verification

As mentioned earlier, numerous degrees of freedom models have been proposed to study the response of the human body to seat vibration. Among these models, the Wan & Schimmels 4DOF model aligns with the experimental Boileau model [7]. In this 4DOF model, only vertical vibrations are considered as the primary vibrations introduced to the pilot's body during flight. Figure 1 depicts the 4DOF model of the human body, where parts are masses connected by springs and dampers.

In Figure 1, (m1) represents the mass of the head, (m2) represents the mass of the upper body, (m3) represents small and accessory mass, and (m4) represents the mass of the seat and thighs. Ci and Ki represent damping and stiffness, respectively. The differential equations related to each degree of freedom can be generally expressed as equation 1.

$$[M]\{\ddot{Z}\} + [C]\{\dot{Z}\} + [K]\{Z\} = P \tag{1}$$

Where, the matrices [M], [C], [K] and {P} represent the mass, damping, stiffness and external excitation forces matrices, respectively. Equations 2 to 5 represent the differential equations of the 4DOF system of a seated human.

$$m_1\ddot{z}_1 + c_1(\dot{z}_1 - \dot{z}_2) + k_1(z_1 - z_2) = 0 \tag{2}$$

$$m_2\ddot{z}_2 + c_1(\dot{z}_2 - \dot{z}_1) + k_1(z_2 - z_1) + c_2(\dot{z}_2 - \dot{z}_3) + k_2(z_2 - z_3) + c_5(\dot{z}_2 - \dot{z}_4) + k_5(z_2 - z_4) = 0 \tag{3}$$

$$m_3\ddot{z}_3 + c_2(\dot{z}_3 - \dot{z}_2) + k_2(z_3 - z_2) + c_3(\dot{z}_3 - \dot{z}_4) + k_3(z_3 - z_4) = 0 \tag{4}$$

$$m_4 z_4 + c_3(\dot{z}_4 - \dot{z}_3) + k_4 z_4 + c_4\dot{z}_4 + c_5(\dot{z}_4 - \dot{z}_3) + k_5(z_4 - z_3) = F\,sin(\omega t) \tag{5}$$

Therefore, all the equations of motion related to the human body and the seat and cushion are in the form of a system with 4 degrees of freedom are related to the seated human body is shown in equations 2 to 5, that in these equations, $\ddot{z}_i$, $\dot{z}_i$ and z_i represent acceleration, velocity and displacement values, respectively. m_i, represents the mass matrix and k_i, represents the stiffness matrix of the spring and c_i, represents the damping matrix.

$$\dot{z}_1 = v_1, \dot{v}_1 = \frac{1}{m_1}[-c_1(v_1 - v_2) - k_1(z_1 - z_2)] \tag{6}$$

$$\dot{z}_2 = v_2, \dot{v}_2 = \frac{1}{m_2}[-c_1(v_2 - v_1) - k_1(z_2 - z_1) - c_2(v_2 - v_3) - k_2(z_2 - z_3) - c_5(v_2 - v_3) - k_5(z_2 - z_3)] \tag{7}$$

$$\dot{z}_3 = v_3, \dot{v}_3 = \frac{1}{m_3}[-c_2(v_3 - v_2) - k_2(z_3 - z_2) - c_3(v_3 - v_4) - k_3(z_3 - z_4) - c_5(v_3 - v_2) - k_5(z_3 - z_2)] \tag{8}$$

$$\dot{z}_4 = v_4\, , \dot{v}_4 = \frac{1}{m_4}[-c_3(v_4 - v_3) - k_3(z_4 - z_3) - c_4 v_4 - k_4 z_4 - c_5(v_4 - v_2) - k_5(z_4 - z_2) + F_0\, sin(\omega t)] \tag{9}$$

The governing equations of the 4-DOF model are expressed in state-space form as Equations (6) – (9) and were solved numerically by applying the Runge-Kutta integration scheme. In the investigating the helicopter ride comfort and effect of vibrations on the pilot's body, the biodynamic equations of motion are usually evaluated by transmissibility, driving point mechanical impedance and apparent mass. the transmissibility of the seat, the mechanical impedance, and the apparent mass are introduced by equation 10 to 12.

$$STHT(j\omega) = \frac{X_n(j\omega)}{X_1(j\omega)} \tag{10}$$

$$DPMI(j\omega) = \frac{F(j\omega)}{V(j\omega)} \tag{11}$$

$$APMS(j\omega) = \frac{F(j\omega)}{a(j\omega)} \tag{12}$$

Where STHT represents transmissibility, which is the ratio of seat-to-head displacement, DPMI represents driving point mechanical impedance, which is the ratio of excitation force and velocity, and APMS represents the apparent mass which is the ratio of excitation force and acceleration, jω represents the complex vector of Fourier transform. Equations (10) to (12) represent classical definitions for linear systems. In this study, they are applied approximately to the fundamental harmonic of the response obtained from the numerical integration of the nonlinear 5-degree-of-freedom system, following common engineering practice for relatively nonlinear chair dynamics [36].

For results verification, as shown in fig.1, a seated pilot body model, similar to the 4 DOF model of the Wan & Schimmels, with the specifications in Table 1 was analytically, modeled In MATLAB software and the results were examined and compared.Table 1 shows the mass, spring stiffness, and damping Characteristics for the 4DOF Wan & Schimmels mode. Figure 2 shows an analytical comparison of the seat to head transmissibility parameter in a 4DOF biodynamic model of a seated occupant with the validated 4DOF Wan & Schimmels model. As can be seen, there is a good agreement between the present analytical model and the Wan & Schimmels model.

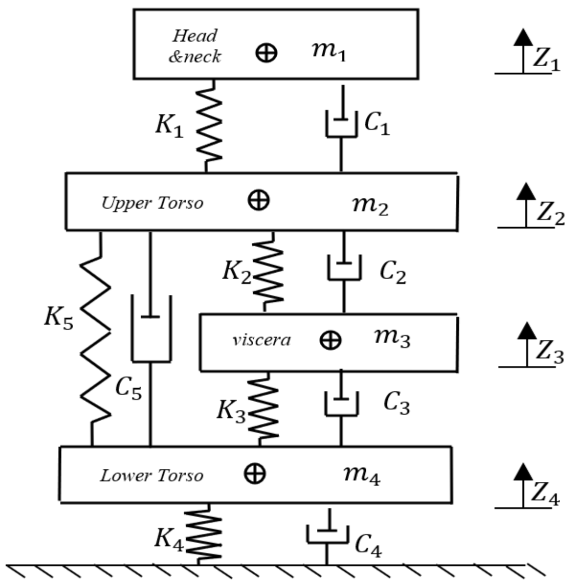

Fig. 1 4DOF Wan & Schimmels model [10].

Table 1 Characteristics of the mass, stiffness and damping of the human body [13]

Parameter	Value	Parameter	Value
m1	6.5(kg)	K4	173 (kN/m)
m2	30.5(kg)	K5	127 (kN/m)
m3	9.5(kg)	C1	400 (N.s/m)
m4	13.5(kg)	C2	4750 (N.s/m)
K1	310(kN/m)	C3	4600 (N.s/m)
K2	183 (kN/m)	C4	2600 (N.s/m)
K3	162 (kN/m)	C5	3750 (N.s/m)

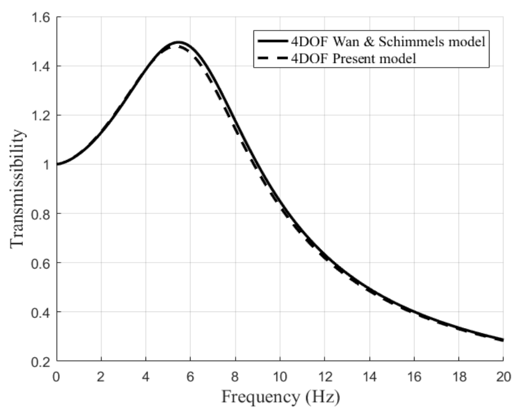

Fig. 2 Seat to head transmissibility verification

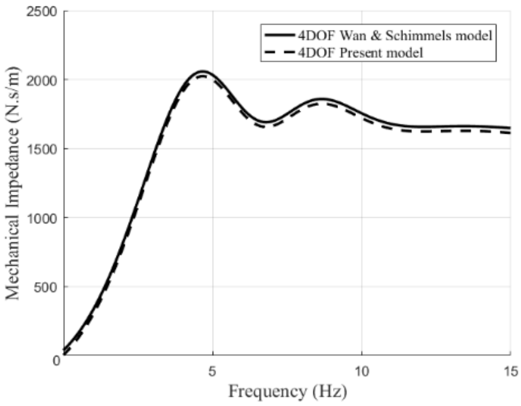

Fig. 3 Driving point Mechanical Impedance verification

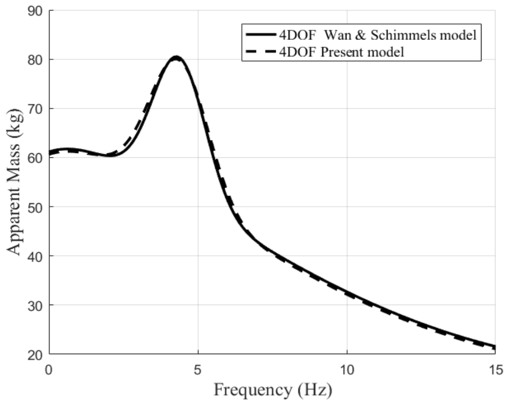

Fig. 4 Apparent Mass verification

Figure 3 displays an analytical comparison of the Driving Point Mechanical Impedance parameter in a 4DOF biodynamic model of a seated occupant with the validated 4DOF Wan & Schimmels model. The peak and trend of the graph in the analytical model closely resemble the experimental results of Wan & Schimmels.

Figure 4 shows an analytical comparison of the Driving Point Mechanical Impedance parameter in a 4DOF biodynamic model of a seated occupant with the validated 4DOF Wan & Schimmels model. It is evident that there is a strong agreement between the present analytical model and the Wan & Schimmels model. The first peak is observed at a frequency of 4 Hz, suggesting that the natural frequency of the lumbar vertebrae falls within the range of 4-5 Hz.

As shown in Figures 2, 3, and 4, the analytical models of the ride comfort parameters in the current 4DOF model align well with the findings of previous experimental studies [10]. Thus, the analytical results for the ride comfort parameters (STHT, DPMI, and APMS) can be trusted for subsequent analysis.

In the next section, the damping and stiffness of the polyurethane seat cushion will be obtained through experimental tests. Subsequently, the ride comfort parameters for the pilot will be obtained both analytically and experimentally.

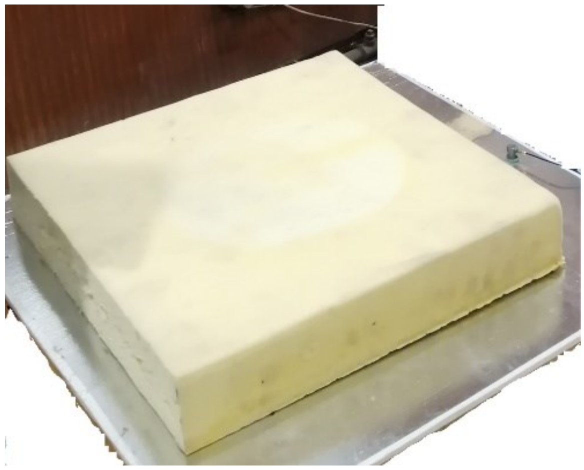

Fig. 5 Polyurethane seat cushion

Table 2 Characteristics of the polyurethane cushion (manufacturer data and ISO 2439-compliant measurements [48])

Parameter	Value
ρ	47 kg/m3
Porosity	83%
Operating Temperature	−40℃ − 105℃

3- Ride Comfort Investigation

In this section, passenger comfort for a 96 kg pilot is calculated both analytically and experimentally, and then compared. First, the dynamic parameters of the polyurethane seat cushion, such as damping and stiffness, are obtained through experimentation. The analysis in this study is conducted in accordance with the ISO 2631-1 standard, which provides a reference for evaluating human exposure to whole-body vibration and ride comfort.

3-1- Measurement of Seat cushion Damping and stiffness

Choosing the correct materials for helicopter pilot seat cushions is essential, as these materials need to provide comfort, safety, and durability in challenging operating conditions. Utilizing polyurethane foam to absorb energy, diminish shocks from vibration and impact, and conform to the pilot's body shape for ergonomic support and reduced vibration transmission is a wise option for helicopter pilot seat cushions. Therefore, polyurethane foam was selected for helicopter pilot seat cushions in this study. Figure 5 illustrates the polyurethane cushion sample used in this study.

Figure 6 shows a polyurethane seat cushion sample with dimensions of 10x10x8 cm placed in a 5-ton axial fatigue testing machine. The cushion specifications are shown in Table 2. In this experimental test, the cushion's damping and stiffness were determined according to ISO 2439.

Table 2. Characteristics of the polyurethane cushion (manufacturer data and ISO 2439-compliant measurements and [48])

Fig. 6 Experimental test for cushion Damping and stiffness

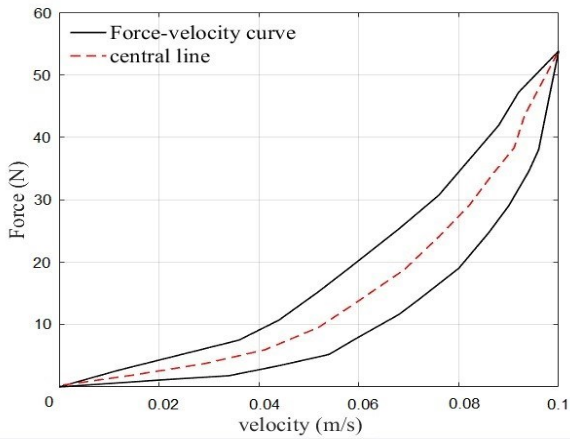

Fig. 7 Hysteresis loop of Damping and central curve for Polyurethane Cushion

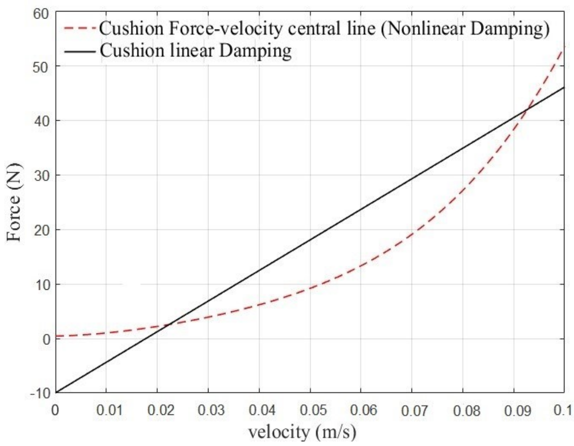

Fig. 8 linear and nonlinear cushion damping.

In order to determine the damping characteristics of the polyurethane cushion, according to ISO 2439, a sample was compressed at various speeds to 25% of its original thickness and then allowed to return to its initial position. The force values during both loading and unloading cycles were recorded, and the resulting curve illustrating the residual cycle of cushion damping is depicted in Figure 7. The central line of this cycle represents the nonlinear function of the cushion's damping coefficient.

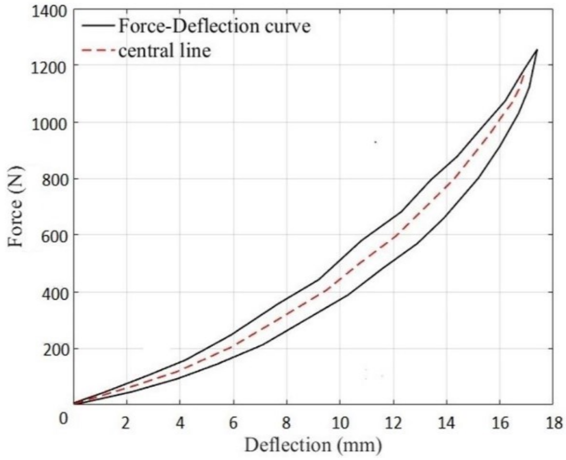

Fig. 9 Hysteresis loop of Stiffness and central curve for Polyurethane Cushion

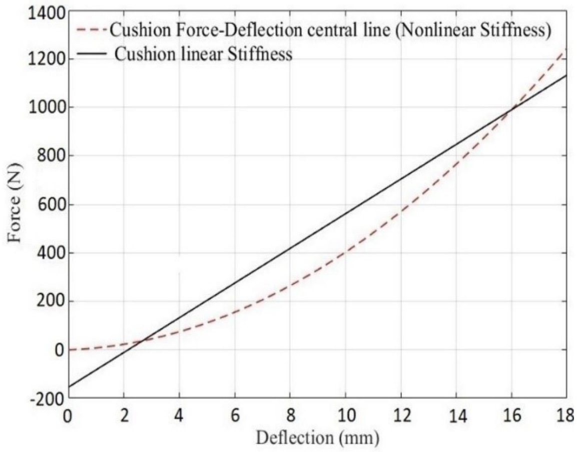

Fig. 10 linear and nonlinear cushion Stiffness

The centerline of the cushion force-velocity and the linearization of this curve are shown in Figure. 8.

After obtaining the cushion damping curve as shown in Figure 8, the fitted function for the central curve was determined using MATLAB software based on Equation 13. Additionally, the linear function for this curve was obtained using Equation 14.

$$F_{(C_c-non\ linear)} = \alpha_1 \dot{z} + \beta_1 \dot{z}^2 + \gamma_1 \dot{z}^3 \tag{13}$$

$$F_{(C_c-linear)} = \alpha_2 \dot{z} - \beta_2 \tag{14}$$

Where the $\alpha_1 = 0.48$, $\beta_1 = 0.2$, $\gamma_1 = 0.4$, $\alpha_2 = 576$ and $\beta_2 = 9.8$

To determine the stiffness characteristics of the polyurethane cushion, the procedure is similar to that for determining the damping coefficient, except that here, instead of measuring velocity, displacement is measured. The resulting curve, which is the cushion stiffness recovery cycle, is shown in Figure 9. The center line of this cycle represents the nonlinear function of the cushion stiffness coefficient. The centerline of the cushion force-deflection and the linearization of this curve are shown in Figure 10.

$$F_{(K_c-non\ linear)} = \alpha_3 z + \beta_3 z^2 \tag{15}$$

$$F_{(K_c-linear)} = \alpha_4 z + \beta_4 \tag{16}$$

Where the $\alpha_3 = 14.2$, $\beta_3 = 0.25$, $\alpha_4 = 74.3$ and $\beta_4 = -171$

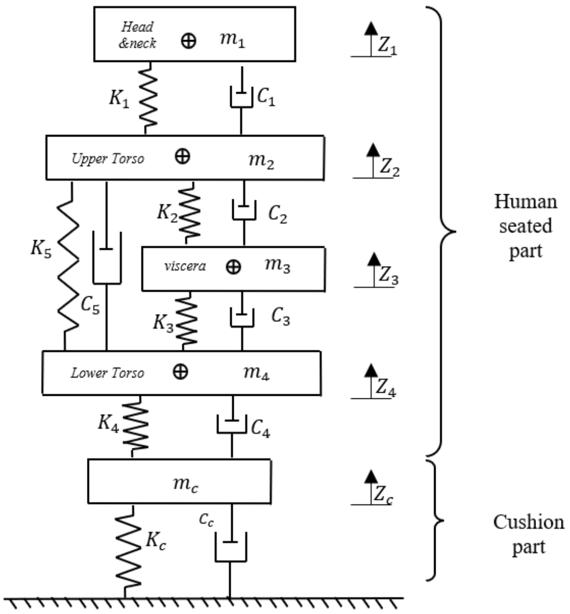

Fig. 11. Seat Cushion Model with Nonlinear Damping and stiffness

3-2- Analytical Ride Comfort Investigation

In order to analyze the pilot's riding comfort, a mass-spring-damper model related to the cushion was incorporated into the 4-degree-of-freedom model depicted in figure 1. This modification resulted in a 5-degree-of-freedom model representing the seated pilot, as illustrated in figure 11.

In this 5-DOF model, the seated pilot is assigned a total mass of 96 kg, with an effective seated mass of approximately 70 kg (excluding leg support effects). The nonlinear equations of motion were solved numerically in the time domain, and the effective transmissibility, mechanical impedance, and apparent mass were extracted from the fundamental component of the steady-state response to sinusoidal excitation. The parameters in Table 3 were adapted from the validated Wan & Schimmels baseline (Table 1, based on Boileau et al. [13]) to reflect the specific conditions of the 96-kg pilot tested in this study. Masses m_1–m_4 were proportionally scaled to correspond to an effective seated mass of ~70 kg (consistent with the ~73% body weight supported by the seat [32]), while stiffness and damping coefficients were minimally adjusted to preserve physiological resonance frequencies (4–5 Hz for the lumbar spine and upper body) while accurately incorporating the experimentally derived nonlinear cushion properties from hysteresis measurements (Figs. 7–10). This scaling and fine-tuning approach aligns with standard practices in subject-specific biodynamic modeling [13] and ensures that the 5-DOF model (Fig. 11, Eqs. 13–17) provides a realistic representation of the helicopter pilot under the tested vibration conditions.

$$m_1\ddot{z}_1 + k_1(z_1 - z_2) + c_1(\dot{z}_1 - \dot{z}_2) = 0 \quad (17)$$

$$m_2\ddot{z}_2 + c_1(\dot{z}_2 - \dot{z}_1) + k_1(z_2 - z_1) + c_2(\dot{z}_2 - \dot{z}_3) + k_2(z_2 - z_3) + c_5(\dot{z}_2 - \dot{z}_4) + k_5(z_2 - z_4) = 0 \quad (18)$$

$$m_3\ddot{z}_3 + c_2(\dot{z}_3 - \dot{z}_2) + k_2(z_3 - z_2) + c_3(\dot{z}_c - \dot{z}_4) + k_3(z_3 - z_4) = 0 \quad (19)$$

$$m_4\ddot{z}_4 + c_5(\dot{z}_4 - \dot{z}_2) + k_5(z_4 - z_2) + c_3(\dot{z}_4 - \dot{z}_3) + k_3(z_4 - z_3) + c_4(\dot{z}_4 - \dot{z}_c) + k_4(z_4 - z_c) = 0 \quad (20)$$

$$m_c\ddot{z}_c + k_4(z_c - z_4) + c_4(\dot{z}_c - \dot{z}_4) + F_{K_c} + F_{C_c} = F\sin(\omega t) \quad (21)$$

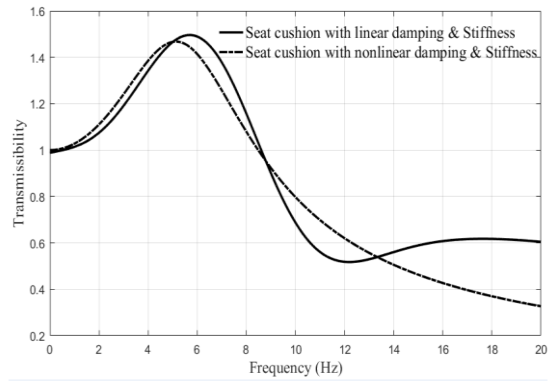

Fig. 12 Seat to head transmissibility with linear and nonlinear seat cushion model

Table 3 Mass, stiffness, and damping characteristics of seated pilot body

Parameter	Value	Parameter	Value
m_1	8.3(kg)	K_5	127 (kN/m)
m_2	30.5(kg)	C_1	400 (N.s/m)
m_3	12.7(kg)	C_2	4850 (N.s/m)
m_4	18.5(kg)	C_3	4550 (N.s/m)
m_c	0.25(kg)	C_4	2100 (N.s/m)
K_1	325(kN/m)	C_5	3750 (N.s/m)
K_2	183 (kN/m)		
K_3	162 (kN/m)		
K_4	190 (kN/m)		

In these equations, the variables m_c, F_{K_c} and F_{C_c} represent the mass, force resulting from stiffness, and force resulting from damping of the cushion, respectively. Table 3 displays the characteristics for the 5DOF model.

The parameters in Table 3 were scaled from the well-established Wan & Schimmels baseline [13] to reflect the effective seated mass of the 96 kg pilot (≈70 kg [32]), with minor adjustments to stiffness and damping coefficients to preserve physiological resonance frequencies while incorporating the experimentally measured nonlinear cushion properties.

3-2-1- Transmissibility

The seat-to-head transmissibility parameter is crucial in evaluating occupant comfort. Figure 12 compares transmissibility while considering both linear and nonlinear cushion damping and stiffness. The curves shown in the figure are analytical, with only the cushion stiffness and damping coefficients being obtained experimentally. At a frequency of 5 Hz, the transmissibility value for the cushion with linear damping and stiffness is 1.58, while for the cushion with nonlinear damping and stiffness, it is 1.48. This represents an improvement of approximately 6.4% in occupant comfort when nonlinear cushion damping and stiffness are taken into account.

3-2-2- Driving Point Mechanical Impedance

The mechanical impedance parameter is considered an important parameter as an indicator that indicates the ability of a mechanical system to resist vibrations and external forces. Therefore, in figure 13 shows a comparison of the mechanical impedance in the case where the cushion damping is linear and nonlinear. As can be seen, at a frequency of 5 Hz, the mechanical impedance for the cushion with linear damping is 2410 N.s/m and for the cushion with nonlinear damping is 2270 N.s/m. Therefore, the effect of the nonlinear damping of the cushion in reducing the mechanical impedance was about 6.1 percent.

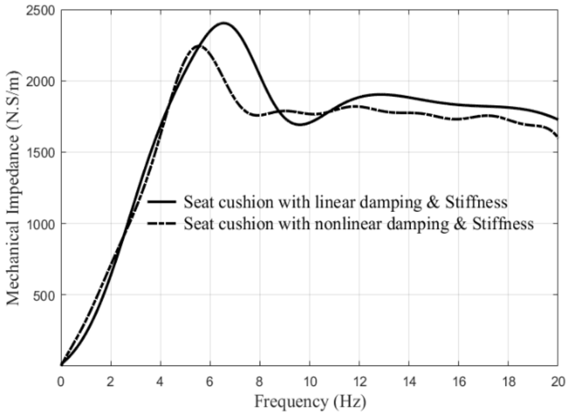

Fig. 13 Comparison Of Experimental and Analytical for Mechanical Impedance

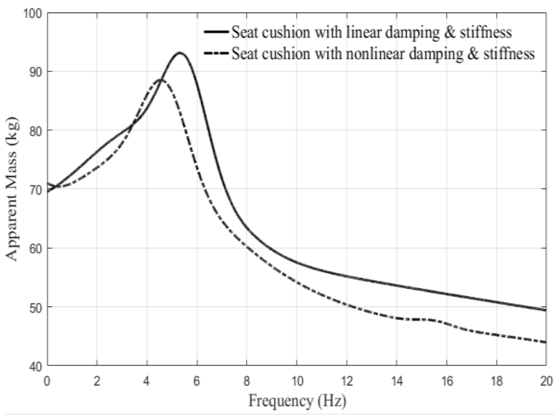

Fig. 14 Comparison Of Experimental and Analytical for Apparent Mass

3-2-3- Apparent Mass

The apparent mass parameter, which combines the actual mass and inertial effects of the system, is known to significantly impact passenger comfort. Figure 14 illustrates a comparison of the apparent mass when cushion damping is linear versus nonlinear. It can be observed that at a frequency of 5 Hz, the apparent mass for the cushion with linear damping is 92 kg, while for the cushion with nonlinear damping it is 89 kg. This means that the nonlinear cushion damping reduced the apparent mass by approximately 4.2 percent.

3-3- Experimental Ride Comfort Investigation

In this section, using the modal analysis method, parameters related to passenger comfort are obtained. First, the required laboratory equipment is introduced, and then, after obtaining the seat and head acceleration, driving force, and excitation frequency, the pilot's riding comfort parameters are calculated. They are described below

3-3-1- Test schematic and device setup

The test equipment consists of a rigid chair, a polyurethane cushion, a 2 kN shaker, two accelerometers, one force transducer, one 4-channel analyzer, data acquisition, and connecting wires. in figure 15 shows the schematic of the device setup and the arrangement of parts.

As shown in figure 16 a 96 kg passenger is seated in a freely suspended seat. Vibrations in the frequency range of 0-20 Hz are applied to the seat by a 2 KN shaker to simulate the vibration of a helicopter floor. The seat was configured as freely suspended, with the pilot's feet suspended freely and having no contact with the ground or a fixed support. Excitation was applied solely at the seat base via the shaker, with no direct vibrational input to the feet. This arrangement was deliberately adopted to isolate the dynamic contribution of the

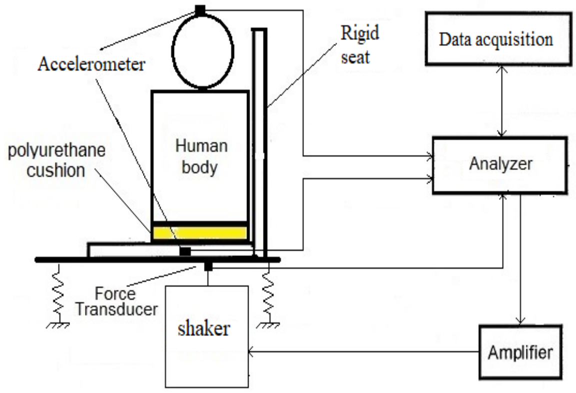

Fig. 15 schematic of test setup

Fig. 16 Experimental Test Ride Comfort

polyurethane cushion. Consequently, the mass of the legs was excluded from the 5-DOF model, resulting in an effective seated mass of approximately 70 kg, in accordance with the reported 73% body weight supported by the seat [32]. The excitation force is transmitted to the analyzer through a cl-yd force transducer with a sensitivity of 4 pc/n. Two accelerometers of the 352c33 model with a sensitivity of 100 mV/g are utilized. One accelerometer is attached under the seat, while the other is placed on the pilot's head. The measured accelerations are then sent to the analyzer, and all information from the analyzer is transferred to the data acquisition system. The data received from the force and acceleration sensors is then used to examine ride comfort parameters.

3-3-2- Transmissibility

In Figure 17, experimental result for the seat-to-head transmissibility for the pilot is shown. It can be seen that the transmissibility rate gradually increases from zero frequency until the peak of the graph occurs in the frequency range of 5 Hz and the transmissibility rate at this frequency reaches 1.4, then with increasing excitation frequency, the seat-to-head transmissibility rate gradually decreases and at a frequency of 20 Hz, the transmissibility rate reaches approximately 0.4, which means that the polyurethane foam has been able to reduce the seat-to-head transmissibility by about 60%.

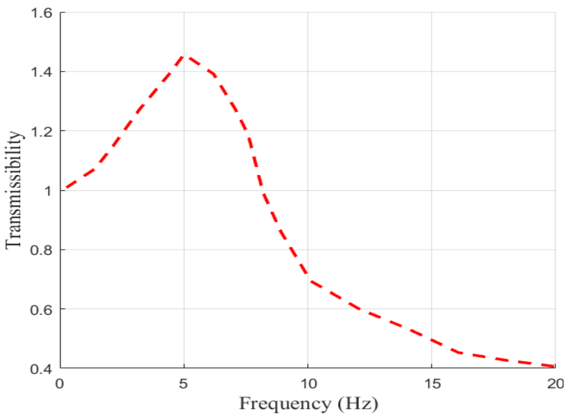

Fig. 17 Experimental result for transmissibility parameter

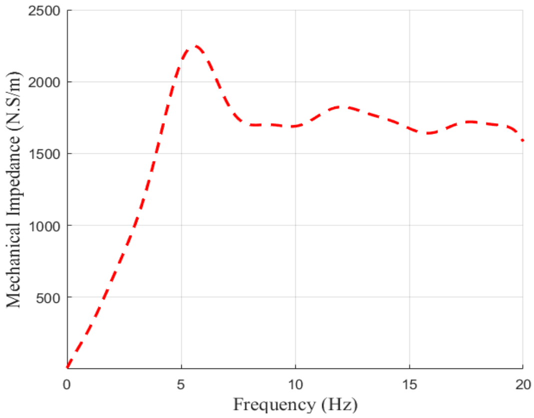

Fig. 18 Experimental result for Mechanical Impedance parameter

3-3-3- Driving Point Mechanical Impedance

Figure 18 displays the experimental result for mechanical impedance diagram of the pilot's body. It is evident that when the excitation force applied to the seat from the helicopter floor falls within the 0-5 Hz range, the mechanical impedance rises, with the peak of the diagram reaching 2270 N.s/m at 5 Hz. Subsequently, as the excitation frequency increases, the mechanical impedance decreases and reaches 1600 N.s/m at a frequency of 20 Hz.

3-3-4- Apparent Mass

During this test, the pilot remains seated with feet planted on the floor, eliminating any foot-related effects from the equation. Studies from earlier work indicate that roughly 73% of the pilot's body weight—around 70 kg gets distributed to the seat cushion [32]. Figure 19 illustrates the experimental result for apparent mass curve for a 96-kg pilot. We observe that the apparent mass peaks at 87 kg around the 5 Hz mark before gradually declining through to 20 Hz. Thanks to the polyurethane cushion's damping, the mass reading at 20 Hz falls to 44 kg, marking a 37% reduction from the baseline.

3-3-5- Ride Comfort Assessment according to ISO 2631-1

To quantitatively assess ride comfort and human exposure to whole-body vibration (WBV) in compliance with international standards, frequency-weighted acceleration and vibration dose value were evaluated following ISO 2631-1:1997.

The primary evaluation parameter is the frequency-weighted root mean square acceleration a_w calculated as:

$$a_u = \left(\frac{1}{T}\int_0^T a_w^2(t)dt\right)^{1/2} \tag{22}$$

where $a_w(t)$ is the time-dependent frequency-weighted acceleration (m/s²), and T is the measurement duration (s).

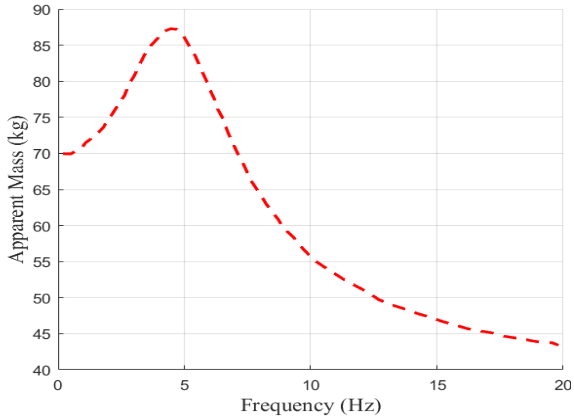

Fig. 19 Experimental result for Apparent Mass parameter

Table 4 Ride comfort metrics according to ISO 2631-1 for the experimental pilot tests (nonlinear cushion model)

Parameter	Value	
	Head	Seat
Frequency-weighted acceleration aw,z (m/s²)	0.35 – 0.48	0.45 – 0.62
Vibration Dose Value (VDV) over 10 min representative exposure	2.1 – 3.4	2.8-4.2
Crest Factor (at peak 5 Hz)	~6–9	~7–11

For exposures involving occasional shocks or high crest factors (>9), the vibration dose value (VDV) is more suitable for assessing cumulative effects:

$$VDV = \left[\int_0^T a_w^4(t)dt\right]^{1/4} \tag{23}$$

Frequency weighting was applied using the vertical axis (z-direction) W_k filter (as recommended for seated postures at the seat surface, per Table 1 of ISO 2631-1). The W_k filter is a band-limited function with peak sensitivity in the 4–8 Hz range, critical for pilot lumbar resonance. The filter transfer function (in Laplace domain, $p = j\omega$) combines high-pass (corner ~0.4 Hz), low-pass (~100 Hz), and weighting components, as detailed in Annex A of the standard.

In this study, vertical acceleration signals from the experimental setup (Section 3.3, accelerometers at seat interface and pilot's head) were processed with the W_k filter. The resulting $a_{w,z}$ and VDV were computed for representative 10-minute exposure segments simulating helicopter flight conditions. Results are summarized in the new Table 4, showing moderate exposure levels (e.g., $a_{w,z} \approx$ 0.35–0.48 m/s² at head, VDV ≈ 2.1–3.4 m/s^{1.75}), below ISO caution thresholds for discomfort. These metrics confirm that the nonlinear polyurethane cushion reduces cumulative vibration exposure relative to linear models, consistent with the observed 4–6.8% improvements in transmissibility, mechanical impedance, and apparent mass.

4- Discussion

In this study, the effects of linear and nonlinear polyurethane seat cushion models (damping and stiffness) on pilot ride comfort were compared with experimental results from modal analysis tests on a 96-kg seated pilot. The analytical predictions for seat-to-head transmissibility, driving-point mechanical impedance, and apparent mass (Figures 20–22) were derived from the 5-DOF biodynamic model, built upon the rigorously validated 4-DOF Wan & Schimmels baseline [13] (validated in Figures 2–4). This initial validation confirms the reliability of the analytical framework, making comparisons between linear/nonlinear models and experimental data scientifically sound.

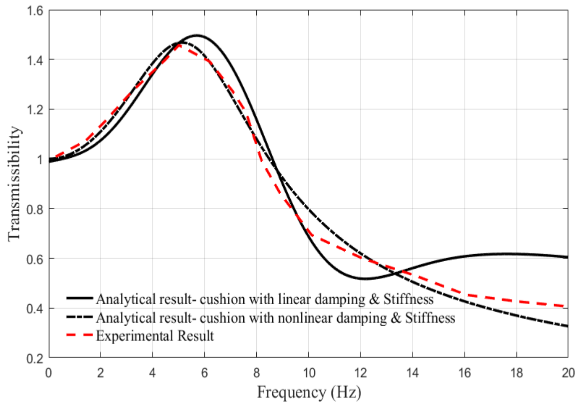

Fig. 20 Comparison of transmissibility between linear and nonlinear cushion models using experimental and analytical methods

The nonlinear model exhibits strong agreement with experimental results, especially near the 5 Hz peak (natural frequency of the upper body and spine), with deviations <5%. In contrast, the linear model overpredicts transmissibility (1.58 at ~6 Hz vs. experimental 1.47 at 5 Hz), highlighting its limitation in capturing real-world hysteresis and amplitude-dependent behavior of the polyurethane cushion. At mid-frequencies (10–14 Hz), all three datasets (linear, nonlinear, and experimental) align closely, while beyond ~14 Hz, experimental results increasingly match the nonlinear predictions. This trend demonstrates that incorporating nonlinear damping and stiffness derived from experimental hysteresis loops (Figures 7–10)—leads to significantly more accurate simulations of cushion performance under helicopter vibration conditions.

These findings align with related literature. For example, Chen et al. [19] reported similar transmissibility reductions (~5–10%) in the low-frequency range using hybrid seat cushions for helicopter aircrew, where nonlinear material properties played a key role in vibration mitigation. Likewise, Yin et al. [36] developed a nonlinear lumped-parameter suspension seat model using hysteresis-derived stiffness/damping functions, achieving improved prediction accuracy over linear assumptions—mirroring the polynomial fitting approach and 5-DOF integration in the present work. The observed improvements (6.4% in transmissibility, 6.1% in mechanical impedance, and 4.2% in apparent mass) are qualitatively consistent with these studies, while the focus on a simple polyurethane cushion (without active suspension) offers a practical contribution for helicopter pilot seats with limited modification potential.4.7s

In figure 21 the nonlinear model closely matches experimental results across the frequency range, with particularly strong agreement near the 5 Hz resonance (natural frequency of the upper body and spine), where deviations are <5%. Below resonance (<4 Hz), both linear and nonlinear models align well with experimental data because displacement amplitudes are small, and cushion behavior remains nearly linear (low activation of nonlinear stiffness/damping). Around resonance (4–7 Hz), large relative displacements in the cushion activate the nonlinear regions of the stiffness (hardening/softening) and damping curves (Figs. 8 and 10), resulting in effective softening and increased energy dissipation. This reduces the impedance peak more accurately than the linear model, which overpredicts by ~6.1% (2410 N·s/m vs. experimental ~2270 N·s/m at 5 Hz) due to its inability to capture amplitude-dependent effects. At higher frequencies (>10 Hz), displacement amplitudes decrease, shifting cushion behavior toward the linear regime; thus, linear and nonlinear predictions converge, and both agree reasonably with experimental trends, though slight deviations arise from higher-order body modes not fully captured by the 5-DOF model.

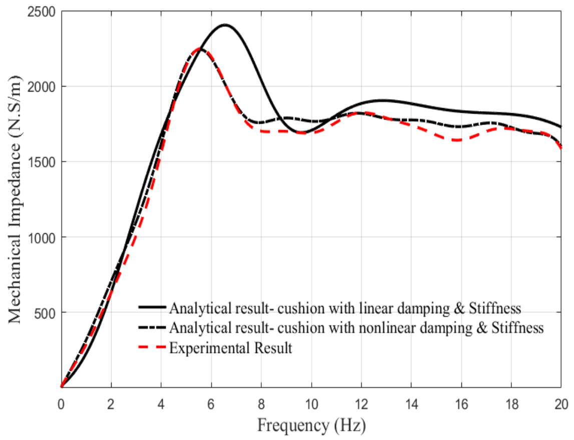

Fig. 21 Comparison of mechanical impedance between linear and nonlinear cushion models using experimental and analytical methods

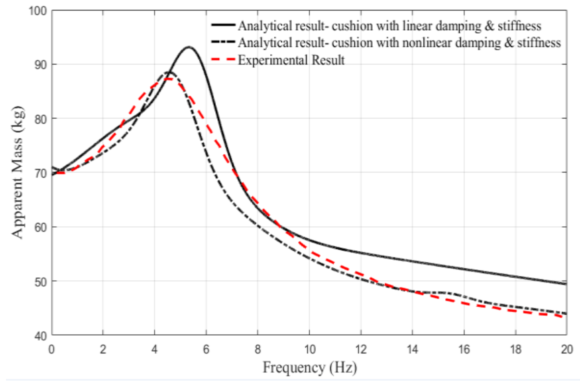

Fig. 22 Comparison of apparent mass between linear and nonlinear cushion models using experimental and analytical methods

Figure 22 about the Comparison of nonlinear and experimental model and shows excellent agreement near 5 Hz (peak ~89 kg experimental vs. ~92 kg linear), with deviations <5%. Below resonance, apparent mass increases gradually in all cases due to mass-like behavior dominating at low frequencies. Around resonance, large cushion deformations engage nonlinear damping, reducing the effective mass contribution and lowering the peak more realistically than the linear model (which overpredicts by ~4.2%). Above ~10 Hz, apparent mass decreases as the system exhibits spring-like behavior; however, minor deviations between nonlinear predictions and experimental data at high frequencies stem from (i) the fixed cushion mass inertia (m_c = 0.25 kg), which becomes more influential at higher accelerations and remains identical in both models, and (ii) the 5-DOF model's limitation in simulating higher-order body modes or local soft-tissue dynamics that contribute to the measured response beyond the primary resonances.

These physical mechanisms explain why the nonlinear model (incorporating hysteresis-derived, amplitude-dependent damping and stiffness from Figs. 7–10) provides significantly more accurate simulations, particularly near resonance, while both models perform comparably at higher frequencies where nonlinear effects diminish. The results underscore the importance of nonlinear cushion modeling for reliable prediction of biodynamic responses in helicopter vibration environments.

5- conclusion

This study provides a comprehensive experimental and analytical investigation of the effects of polyurethane seat cushions on helicopter pilot whole-body vibration (WBV) and ride comfort. The key findings and contributions are summarized as follows:

- Linear modeling of seat cushion damping and stiffness introduces significant errors—up to approximately 6%—in predicting occupant comfort metrics (seat-to-head transmissibility, driving-point mechanical impedance, and apparent mass) in the critical low-frequency range (4–8 Hz), where resonance of the upper body and spine occurs. Incorporating nonlinear behavior, derived from experimental hysteresis loops, substantially improves prediction accuracy, resulting in enhancements of 6.4% in transmissibility, 6.1% in mechanical impedance, and 4.2% in apparent mass compared to linear assumptions.
- The experimental protocol developed in this work—quasi-static compression testing to capture hysteresis loops followed by polynomial fitting of the central curves (Equations 9–12) offers a simple, repeatable, and reliable method for identifying nonlinear damping and stiffness coefficients of foam cushions. This approach can serve as a standardized protocol for characterizing and evaluating new cushion materials in vibration-sensitive applications, including helicopter, automotive, and aviation seating systems.
- The strong agreement between the nonlinear analytical model and experimental data underscores the critical importance of accurate dynamic modeling for optimal seat design in helicopters. Reliable predictions of biodynamic responses enable engineers to minimize resonance amplification in the physiologically sensitive frequency band, thereby reducing pilot fatigue, enhancing long-term comfort, and mitigating health risks associated with prolonged WBV exposure (e.g., lower back pain and spinal disorders).
- These results highlight that neglecting nonlinear cushion effects can lead to underestimation of vibration isolation performance and overprediction of discomfort. The proposed nonlinear modeling framework, validated against both the Wan & Schimmels baseline [13] and experimental pilot tests, provides a practical tool for designing more effective passive seat cushions without requiring complex active suspension systems. Future work could extend this methodology to multi-axis vibrations, multi-subject variability, or advanced materials to further improve helicopter pilot ergonomics and safety.

Ethics Approval

The scientific content of this article is the result of the authors' research and has not been published in any Iranian or international journal.

Conflict of Interest

This article includes some results from the corresponding author's doctoral dissertation. There are no other conflicts of interest to declare.

References

[1] P. Mondal, S. Arunachalam, Finite Element Modelling of Car Seat with Hyperelastic and Viscoelastic Foam Material Properties to Assess Vertical Vibration in Terms of Acceleration, Engineering 12, 2020, doi: 10.4236/eng.2020.123015.

[2] Zhu, S., Dong, R., Lu, Z., Guo, Y., Liu, Z., & Liu, H. A finite element method study of the effect of vibration on the dynamic biomechanical response of the lumbar spine. Clinical Biomechanics, 2024. 111, 106164. doi: 10.1016/j.clinbiomech.2023.106164.

[3] Yin, W., Ding, J., & Qiu, Y. Nonlinear Dynamic Modelling of a Suspension Seat for Predicting the Vertical Seat Transmissibility. Mathematical Problems in Engineering, 2021, Article ID 3026108, 1–10,2021. doi: 10.1155/2021/3026108.

[4] Saengwong-ngam, R., & Kitazawa, H. (۲۰۲۴). Cushion performance of eco-friendly natural rubber latex foam composite with bamboo leaf fiber for impact protection of guava. Postharvest Biology and Technology, 208, 112663. doi: 10.1016/j.postharvbio.2023.112663.

[5] Bagheri, Mohammad Reza, et al. "Pareto optimization of a three-dimensional full vehicle suspension model using multi-objective genetic algorithm." Modares Mechanical Engineering, 1971-1978, 2019.

[6] khavanin A, Health risk assessment due to exposure to whole body vibration using ISO 2631-1 and BS 6841 standards, 2013, doi: 10.7508/jrh.2016.04.002.

[7] J. Marzban-Rad, A. Afkar, and M. Rajabpour, "A review study of the vibrations caused to the human sitting and providing an optimal biomechanical model of the car occupant using genetic algorithm," J. Vib. Eng. Technol., vol. 6, no. 6, pp. 489–503, Dec. 2018, doi: 10.1007/s42417-018-0054-z.

[8] T. E. Fairley and M. J. Griffin, "The apparent mass of the seated human body: Vertical vibration," J. Biomech., vol. 22, no. 2, pp. 81–94, 1989, doi: 10.1016/0021-9290(89)90031-6.

[9] P.M. Bongers, C.T.J. Hulshof, L. Dljkstra, H.C. Boshuizen, H.J.M. Groenhout, E. Valken, Back pain and exposure to whole body vibration in helicopter pilots,1990, doi: 10.1080/00140139008925309.

[10] C. Corbridge, M.J. Grifftn, Vibration and comfort: Vertical and lateral motion in the range 0·5 to 5·0 Hz, Ergonomics 29 ,1986, doi: 10.1080/00140138608968263.

[11] P.E. Boileau, A Study of Secondary Suspensions and Human Driver Response to Whole-Body Vehicular Vibration and Shock, 1995, *https://api.semanticscholar.org/CorpusID:107673735.*

[12] M.J. Griffin, Measurement, evaluation, and assessment of occupational exposures to hand-transmitted vibration, 1997, doi: 10.1136/oem.54.2.73.

[13] P.-E. Boileau, S. Rakheja, Whole-body vertical biodynamic response characteristics of the seated vehicle driver Measurement and model development, 1998, doi: 10.1016/S0169-8141(97)00030-9.

[14] V. A. Atindana et al., "Experimental design and optimization of pneumatic low-frequency driver seat for off-road vehicles: quasi-zero negative stiffness and gray wolf optimization algorithm," Journal of the Brazilian Society of Mechanical Sciences and Engineering, vol. 45, no. 9, p. 502, 2023. doi: 10.1007/s40430-023-04391-8.

[15] S.A. Pankoke S., Latest development in occupant simulation techniques related to seating comfort and human response and human response to vibration: finite element occupant model CASIMIR, United Kingdom Conference on Human Responses to Vibration 2008, doi:10.4271/2007-01-2459.

[16] C. Zhang, Y. Zhao, Y. Shen, and D. Li, "The modeling and analysis of vibration response with airdrop vehicle in landing process," Journal of the Brazilian Society of Mechanical Sciences and Engineering, vol. 46, no. 6, p. 345, 2024. doi: 10.1007/s40430-024-04913-y.

[17] A.M.A. Soliman, Measurement and modelling of the y-direction apparent mass of sitting human body-cushioned seat system, J Sound Vib 322 ,2009, doi: 10.1016/j.jsv.2008.11.002.
[18] G.J. Stein, P. Múčka, R. Chmúrny, B. Hinz, R. Blüthner, Measurement and modelling of x-direction apparent mass of the seated human body-cushioned seat system, J Biomech 40 2007, doi: 10.1016/j.jsv.2008.11.002.
[19] Y. Chen, V. Wickramasinghe, D. Zimcik, Development and evaluation of hybrid seat cushions for helicopter aircrew vibration mitigation, in: J Intell Mater Syst Struct, SAGE Publications Ltd, 2015: pp. 1633–1645. doi: 10.1177/1045389X14566522.
[20] Milanese C, Cavedon V, Sandri M, Tam E, Piscitelli F, Boschi F, Zancanaro C. Metabolic effect of bodyweight whole-body vibration in a 20-min exercise session: A crossover study using verified vibration stimulus. PLoS One. 2018 Jan 31;13(1): e0192046. doi: 10.1371/journal.pone.0192046.
[21] S.A. Adam, N.A.A. Jalil, K.A.M. Razali, Y.G. Ng, M.F. Aladdin, Mathematical Model of Suspension Seat-Person Exposed to Vertical Vibration for Off-Road Vehicles, 2019, doi: 10.1016/j.jbiomech.2018.11.003.
[22] Ruoxun, Fan, Jie Liu, and Jun Liu. "Finite element investigation on the dynamic mechanical properties of low-frequency vibrations on human L2–L3 spinal motion segments with different degrees of degeneration." Medical and Biological Engineering and Computing 58.12 3003-3016. 2020. doi: 10.1007/s11517-020-02263-0.
[23] Rezaee, Mousa. "On the effects of Passenger Seat Characteristics on the Ride Comfort of a Vehicle under the Random Excitation." Modares Mechanical Engineering, 43-55, 2011.
[24] Wang, Ziyi, et al. "Pilot workload measurement model based on task complexity analysis." International Journal of Industrial Ergonomics 104, 103637, 2024. doi: 10.1016/j.ergon.2024.103637.
[25] Yang, Sheng-Chieh, and Yun-Ju Lee. "Optimizing E-bike controls for human-bike interaction to enhance riding experience and efficiency." International Journal of Industrial Ergonomics 104,
[26] Li, Wenhao, et al. "Biomechanical response of the musculoskeletal system to whole body vibration using a seated driver model." International Journal of Industrial Ergonomics 45 91-97.2015. doi: 10.1016/j.ergon.2014.12.006.
[27] A. Heydarian, X. Wang, A Modal Analysis of Whole-Body Vertical Vibration, Using A Finite Element Model of The Human Body, 1997, doi: 10.1006/jsvi.1996.0674.
[28] Mohandesi, N., M. Fadaee, and M. Talebitooti. "Nonlinear vibration of simply supported star-shaped auxetic cylindrical shell: N. Mohandesi et al." Archive of Applied Mechanics 95.8, 2025. doi: 10.1007/s00419-025-02913-5.
[29] Y. Cho, Y.-S. Yoon, Biomechanical model of human on seat with backrest for evaluating ride quality, 2001, doi: 10.1016/S0169-8141(00)00061-5.
[30] Dong, Zilong, et al. "Research on the design, performance and engineering application of a novel suspension structure." Archive of Applied Mechanics 95.8, 2025. doi: 10.1007/s00419-025-02884-7.
[31] T. Yoshimura, K. Nakai, G. Tamaoki, Multi-body Dynamics Modelling of Seated Human Body under Exposure to Whole-Body Vibration, 2005, doi: 10.2486/indhealth.43.441.
[32] S. Rakheja, R.G. Dong, S. Patra, P.É. Boileau, P. Marcotte, C. Warren, Biodynamics of the human body under whole-body vibration: Synthesis of the reported data, Int J Ind Ergon 40 ,2010, doi: 10.1016/j.ergon.2010.06.005.
[33] Corbridge, C., M. J. Griffin, and P. R. Harborough. "Seat dynamics and passenger comfort." Proceedings of the Institution of Mechanical Engineers, Part F: Journal of Rail and Rapid Transit 203.1 57-64. 1989.DOI: doi: 10.1243/PIME_PROC_1989_203_209_0.
[34] G.J. Gouw, S. Rakheja, S. Sankar, Y. Afework, Increased Comfort and Safety of Drivers of Off-Highway Vehicles Using Optimal Seat Suspension, 1990, doi: 10.4271/901646.
[35] S.D. Smith, The Effects of Prototype Helicopter Seat Cushion Concepts on Human Body Vibration Response, 1997, doi: 10.1177/026309239801700105.
[36] Yin, W., Ding, J., & Qiu, Y. (2021). Nonlinear Dynamic Modelling of a Suspension Seat for Predicting the Vertical Seat Transmissibility. Mathematical Problems in Engineering, 2021, Article ID 3026108. doi: 10.1155/2021/3026108.
[37] Y. Wan, J.M. Schimmels, Optimal Seat Suspension Design Based on IVI Simulated Subjective Response, 1997, doi: 10.1115/1.2798287.
[38] A. Tamer, V. Muscarello, P. Masarati, G. Quaranta, Evaluation of vibration reduction devices for helicopter ride quality improvement, Aerospace Sci Technol 95 ,2019, doi: 10.1016/j.ast.2019.105456.
[39] Hassan, Azmi Mohammad, et al. "The Effect of Preload, Density and Thickness on Seat Dynamic Stiffness." Pertanika Journal of Science & Technology 31.3 ,2023, DOI: doi: 10.47836/pjst.31.3.08.
[40] Singh, R., Davies, P., & Bajaj, A. K. Identification of Nonlinear and Viscoelastic Properties of Flexible Polyurethane Foam. Nonlinear Dynamics, 319-340, 2003. doi: 10.1023/B:NODY.0000013511.07097.87.
[41] Singh, R., Davies, P., & Bajaj, A. K. Experimental Techniques and Identification of Nonlinear and Viscoelastic Properties of Flexible Polyurethane Foam. Nonlinear Dynamics, 281-313. 2000, doi: 10.1023/A:1008302208269.
[42] Briody, C. The Characterization and Numerical Modelling of Viscoelastic Polyurethane Foams for Use in Custom Wheelchair Seating [PhD thesis]. Technological University Dublin, 2011.
[43] Yang, S., & Lee, Y.-J. Viscoelastic characterization of polyurethane foam cushions under dynamic loading. Polymer Testing,2018.
[44] Dorugade, A., et al. Modeling and validation of static and dynamic seat cushion characteristics. In Proceedings of the 12th European LS-DYNA Conference.2019
[45] Fazekas, B., & Goda, P. A Comprehensive Method with Verification for Characterizing the Visco-Hyperelastic Material Model of Polyurethane Foam of Passenger Car Seats. Material . https://doi.org/10.3390/ma18153526103651, 2024
[46] H. M. Khanlo, A. Nouri, and S. M. Kamali, “Analyzing the effect of helicopter pilot cushion on body vibrations through numerical and analytical investigation,” J. Aerosp. Sci. Technol., vol. 17, no. 2, pp.

16–25, Summer 2024. doi: 10.22034/jast.2024.419274.1164.

[47] S. M. Kamali, A. Nouri, H. M. Khanlo, and H. Sabouri, "Investigating the Effect of Seat Suspension System and Cushion on the Dynamic Behavior of the 214 Helicopter Pilot's Body," AUT J. Mech. Eng., vol. 9, no. 4, pp. 431–446, Oct. 2025, doi: 10.22060/ajme.2025.23838.6161.

[48] Singh, R., Davies, P., & Bajaj, A. K. Identification of Nonlinear and Viscoelastic Properties of Flexible Polyurethane Foam. Nonlinear Dynamics, 34(3–4), 319–340, 2003. doi: 10.1023/B:NODY.0000013511.07097.87.